International Journal of Modern Mathematical Sciences, 2016, 14(3): 239-261

International Journal of Modern Mathematical Sciences ISSN:2166-286X

Modern Scientific Press Journal homepage:www.ModernScientificPress.com/Journals/ijmms.aspx Florida, USA

Article

MHD Mixed Convection Chemically Reactive Flow in Radiative Heat Generating Medium with Soret Effect

SanjibSengupta[1,*], AmritKarmakar[2]

[1]*Assam University, Silchar-788011, Assam, India*

[2]*Jawahar Navodaya Vidyalaya, R.C.Ghat-799207, Tripura, India*

* Author to whom correspondence should be addressed; E-Mail: sanjib_aus2009@rediffmail.com, amrit_karmakar@rediffmail.com

Article history: Received 7 March 2016, Received in revised form 8 May 2016, Accepted 20 June 2016, Published 28 July 2016.

Abstract: In this paper an exact analysis is made to study the mixed convective flow of a Newtonian, electrically conducting, incompressible, viscous fluid past a vertical porous plate immersed in heat generating Darcian porous media under the influence of thermal radiation, chemical reaction and thermo- diffusion (Soret) effect. A magnetic field of uniform strength is applied transversely to the plate surface. The Rosseland approximate model is used in the energy equation to quantify the heat flux due to thermal radiation. The governing system of coupled partial differential equations with a set of favorable boundary conditions is transformed to a system of ordinary differential equations by applying a group of asymptotic transformations. The closed form of expressions for the velocity, temperature and concentration fields as well as the skin-friction, Nusselt and Sherwood numbers are obtained in terms of some governed physical parameters. Finally, numerical simulation has been made in terms of graphs and tables. It is observed that, the physical parameters like heat source and Soret number increase the radial velocity of the flow but decrease the Sherwood number. It is also observed that, the Nusselt number as well as the skin-friction decrease due to increase in thermal radiation parameter, while the Sherwood number increases as chemical reaction parameter increases.

Keywords: MHD mixed convection; chemical reaction; thermal radiation; heat generation; Soret effect.

Mathematics Subject Classification 2000: 76D05, 80A20, 82D10

1. Introduction

In the last several years considerable attention has been given to the study of the hydrodynamic thermal convection due to its numerous applications in geophysics and astrophysics. The phenomena of mixed or combined convection arise when both free and forced convection occur simultaneously in a flow system. The transfer of thermal energy which arises due to buoyancy effect is called as free (natural) convection while forced convection results due to any external force. Beckett and Friend (1984) obtained an analytical solution of mixed convective flow between vertical parallel walls for higher Rayleigh number. The problem of mixed convective flow from a wavy surface was presented experimentally by Kuhn and Rohr (2008). In spite of these studies, relatively less attention has been given to the simultaneous effects of the free and forced convection on the hydromagnetic free stream rotating viscous flows past a vertical porous surface. Such work seems to be significant and is required partly for getting a basic understanding of such flows, and partly for possible applications to geophysical and astrophysical problems. Besides the aforesaid study, the interaction of such flow with a magnetic field is important in point of view with the probable applications of many mechanical and electronic devices. Magnetohydrodynamics (MHD) is the study of motion of an electrically conducting fluid in the presence of magnetic field i.e. an electromagnetic field interacting with the velocity field of an electrically conducting fluid. Hydromagnetic flows have become important due to industrial applications, for instance it is used to deal with the problem of cooling of nuclear reactor by fluid having very low Prandtl number. Many liquid metals like Bismuth (Pr = 0.01) and Mercury (Pr = 0.023) etc., with small Prandtl number of order 0.001~0.1, are generally used as coolants because of very high thermal conductivity. On account of their varied importance, these flows have been studied by several authors. Ram (1990) investigated heat and mass transfer on MHD heat generating flow through a porous medium in a rotating fluid. Muthtamilselvan et al. (2014) carried out studies on the effect of non-uniform heat generation on unsteady MHD flow over a vertical stretching surface with variable thermal conductivity.

The role of thermal radiation on the flow and heat transfer process is of significance in the design of many advanced energy conversion systems operating at higher temperatures. Thermal radiation within these systems is usually the result of emission of hot walls and the working fluid. Radiative convective flows are encountered in countless industrial and environment processes e.g., heating and cooling chambers, fossil fuel combustion energy processes, evaporation from large open water reservoirs, astrophysical flow, solar power technology and space vehicle re-entry. Several authors have considered the effect of thermal radiation on Newtonian flows. England and Emery (1969) have studied the thermal

radiation effects on the laminar free convection boundary layer of an absorbing gas. Rajesh and Varma (2010) analyzed radiation effects on MHD flow through a porous medium with variable temperature or variable mass diffusion. Sengupta and Sen (2013) investigated free convective heat and mass transfer flow past an oscillating plate with heat generation, thermal radiation and thermo diffusion effects. Babu et al. (2014) carried out studies on the radiation effect on MHD heat and mass transfer flow over a shrinking sheet with mass suction.

On the other hand, the study of heat and mass transfer problems with chemical reaction is of great practical importance to engineers and scientists because of their almost universal occurrence in many branches of science and engineering. A few representative fields of interest in which combined heat and mass transfer along with chemical reaction play an important role in chemical process industries such as food processing and polymer production. Prakash and Ogulu (2006) were considered the effect of thermal radiation, time-dependent suction and chemical reaction on two-dimensional flow of an incompressible Bousinesque fluid. Chamkha (2003) investigated numerically the MHD flow of an uniformly stretched vertical permeable surface in the presence of heat generation/ absorption and a chemical reaction. Ahmed et al. (2014) worked on the radiation effects of heat and mass transfer over an exponentially accelerated infinite vertical plate with chemical reaction. Imran et al. (2013) carried out the studies on chemical reaction and uniform heat generation or absorption effects on MHD stagnation-point flow of a nano fluid over a porous sheet. Sengupta (2015) has investigated the free convective chemically absorption fluid past an impulsively accelerated plate with thermal radiation, variable wall temperature and concentrations. Sengupta and Ahmed (2015) carried out the studies on chemical reaction interaction on unsteady MHD free convective radiative flow past an oscillating plate embedded in porous media with thermal diffusion. Pal and Talukdar (2011) analyzed the combined effects of Joule heating and chemical reaction on unsteady magnetohydrodynamic mixed convection of a viscous dissipating fluid over a vertical plate in porous media with thermal radiation. Seddeek and Almushigeh (2010) considered the effects of radiation and variable viscosity on MHD free convective flow and mass transfer over a stretching sheet with chemical reaction. SudheerBabu and Satyanarayana (2009) analyzed the effects of the chemical reaction and radiation absorption on free convection flow through porous medium with variable suction in the presence of uniform magnetic field. Kesavaiah et al. (2011) have worked on the effect of the chemical reaction and radiation absorption on an unsteady MHD convective heat and mass transfer flow past a semi-infinite vertical permeable moving plate embedded in a porous medium with heat source and suction.

Many mechanical devices and electronic instruments are there where, heat is generated which causes to minimize the longevity of the devices. Also in particular, in chemical industries as well as in nuclear reactors, huge amount of heat is generated within the medium, which may cause explosion to

the devices. Due to importance of heat generation/absorption in industrial and engineering applications, many researchers have worked on the heat generation/ absorption effect. Bhattacharyya (2011) analyzed the effects of radiation and heat source/sink on unsteady MHD boundary layer flow and heat transfer over a shrinking sheet with suction/injection. Muthtamilselvan et al. (2014) have investigated the effect of non-uniform heat generation on unsteady MHD non-Darcian flow over a vertical stretching surface with variable properties.

It is well known that, the driving potential for the phenomena of transport of mass is not alone concentration gradients, but high temperature gradients as well. The dual process by which mass gets transferred is known as thermo-diffusion or Soret effect. Some of the significant contribution in the study of Soret effect is provided by Raju et al. (2008), Ananda Reddy et al. (2009), Sengupta (2011), Ahmed et al. (2013), Pandya and Shukla (2013), Raju and Verma (2014), Mamatha et al. (2015), Sengupta (2015) and Raju et al. (2016) etc. Very recently, Raju et al. (2016) investigated the Soret effect on unsteady magnetohydrodynamic mixed convection flow in presence of thermal radiation, heat absorption and homogeneous chemically reaction and obtained perturbed solutions for the flow variables.

In the aforesaid studies, the authors have given a minimum amount of attention to the combined effects of heat generation and thermo – diffusion (Soret) effects. The heat that generates in the medium can be utilized to separate heavier components of the species from lighter ones. The objective of the present study is to obtain an exact asymptotic form of solutions for a mixed convective free stream oscillatory flow of Newtonian, incompressible viscous fluid with chemical reaction, thermal radiation and Soret effect in heat generating Darcian porous media in presence of a transverse magnetic field.

2. Basic Equations and Assumptions Considered

2.1. Basic Equations

The vector forms of equations that describe the flow situation are formulated as:

$$\vec{\nabla}.\vec{q} = 0 \qquad \text{(continuity equation)}$$

$$\frac{\partial \vec{q}}{\partial t} + (\vec{q}.\vec{\nabla})\vec{q} = -\frac{1}{\rho}\vec{\nabla}p + \nu\vec{\nabla}^2\vec{q} + \frac{1}{\rho}\vec{J}\times\vec{B} - \frac{\nu}{k}\vec{q} \qquad \text{(MHD Navier-Stokes equation)}$$

$$\rho C_p\left(\frac{\partial T}{\partial t} + (\vec{q}.\vec{\nabla})T\right) = k\vec{\nabla}^2 T - \vec{\nabla}\vec{q}_R + Q^*.\delta T \qquad \text{(Energy equation)}$$

$$\frac{\partial C}{\partial t} + (\vec{q}.\vec{\nabla})C = D_M\vec{\nabla}^2 C + D_T\vec{\nabla}^2 T - K_l\delta C \qquad \text{(Species concentration equation)}$$

$$\vec{J} = \sigma(\vec{E} + \vec{q}\times\vec{B}) \qquad \text{(Ohm's law)}$$

$$\rho_\infty - \rho \approx \rho\beta_T(T^* - T_\infty^*) + \rho\beta_C(C^* - C_\infty^*) \qquad \text{(Modified Boussinesq approximations)}$$

2.2. Basic Assumptions

The fundamental assumptions considered for the study are as follows:

a) All the fluid properties except possibly the pressure are independent of variations of x*-scale.

b) The temperature as well as concentration of fluid particles near the plate surface is supposed to be more than their respective components at the free stream region.

c) The strength of the applied magnetic field, which is applied perpendicular to the plate, considered as moderate and constant. As the value of the magnetic Reynolds number (ratio of the induced magnetic field to applied magnetic field) is very small in comparison to the strength of the applied magnetic field, as such the induced magnetic field effect is found to be negligible and not considered for this study.

d)The polarization of charges is negligible as such the voltage differences at the end of the plate is less and thus the influence of the electric field is also not considered for this study.

e) Due to moderate strength of the magnetic field the viscous dissipation and Joule heating effects are not considered for this study.

3. Mathematical Formulation of the Problem

A co-ordinate system (x*, y*) has been introduce, with its x*-axis along the length of the plate in the upward vertical direction and y*-axis perpendicular to the plate towards the fluid region. A uniform magnetic field of strength B_0 is applied transversely to the plate along the positive direction of y*-axis.

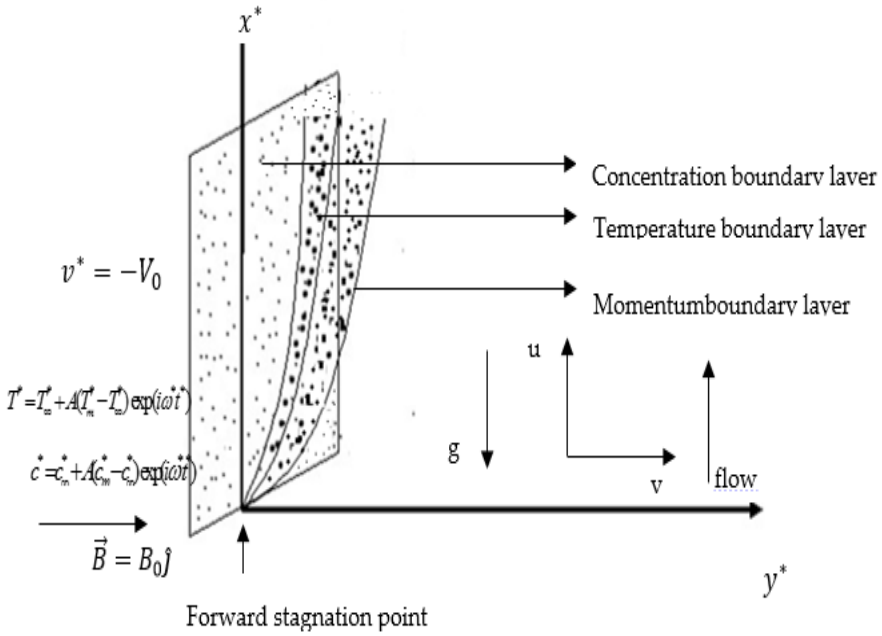

Figure 1: A Schematic representation of the flow configuration and geometry

A semi two - dimensional boundary layer fluid model has been developed in terms of a system of coupled partial differential equations combined with initio-boundary conditions as:

Continuity Equation:

$$\frac{\partial v^*}{\partial y^*} = 0 \tag{1}$$

Momentum Equation:

$$\frac{\partial u^*}{\partial t^*} + v^* \frac{\partial u^*}{\partial y^*} = -\frac{1}{\rho}\frac{\partial p^*}{\partial x^*} + \nu \frac{\partial^2 u^*}{\partial y^{*2}} + g\beta_T (T^* - T_\infty^*) + g\beta_C (C^* - C_\infty^*) - \left(\frac{\sigma B^2{}_0}{\rho} + \frac{\upsilon}{K^*}\right) u^* \tag{2}$$

Energy Equation:

$$\frac{\partial T^*}{\partial t^*} + v^* \frac{\partial T^*}{\partial y^*} = \frac{k}{\rho C_p}\frac{\partial^2 T^*}{\partial y^{*2}} - \frac{1}{\rho C_p}\frac{\partial q^*_{ry^*}}{\partial y^*} + \frac{Q^*}{\rho C_p}(T^* - T_\infty^*) \tag{3}$$

Concentration Equation:

$$\frac{\partial C^*}{\partial t^*} + v^* \frac{\partial C^*}{\partial y^*} = D_M \frac{\partial^2 C^*}{\partial y^{*2}} + D_T \frac{\partial^2 T^*}{\partial y^{*2}} - K_l^* (C^* - C_\infty^*) \tag{4}$$

With initio - boundary conditions as:

$$\left.\begin{array}{l} u^* = 0, T^* = T^*_\infty, C^* = C^*_\infty \text{ for every } y^* \text{ and } t^* \le 0 \\ u^* = 0, T^* = T^*_\infty + A(T^*_m - T^*_\infty)\exp(i\omega^* t^*) \\ C^* = C^* + A(C^* - C^*_\infty)\exp(i\omega^* t^*), \text{ at } y^* = 0 \text{ when } t^* > 0 \\ u^* \to u^*_\infty = A\exp(i\omega^* t^*), T^* \to T_\infty \,\&\, C^* \to C^*_\infty \text{ for } y^* \to \infty, \text{when } t^* > 0 \end{array}\right\} \tag{5}$$

The Rosseland approximation model quantifies the radiative heat flux for an optically thick boundary layer flow in a simplified differential form due to Magyari and Pentokratoras (2011) is considered as:

$$q^*_{ry^*} = -\frac{4\sigma_1}{3k_1}\frac{\partial T^{*4}}{\partial y^*} \tag{6}$$

where, σ_1 and k_1 are the Stefan-Boltzmann constant and Rosseland mean absorption coefficient, respectively. Assuming that the temperature differences within the flow are sufficiently small, so T^{*4} may be expressed as a linear function of temperature T^* and expanding T^{*4} in Taylor's series about T_∞^* and neglecting higher order terms we thus derive,

$$T^{*4} \approx T_\infty^{*4} + (T^* - T^*_\infty)4T_\infty^{*3} = 4T_\infty^{*3}T^* - 3T_\infty^{*4} \tag{7}$$

Using (7) in (6) and finally using in equation (3) gives,

$$\frac{\partial T^*}{\partial t^*} + v^* \frac{\partial T^*}{\partial y^*} = \frac{k}{\rho c_p}\left(\frac{\partial^2 T^*}{\partial y^{*2}}\right) + \frac{16\sigma_1 T_\infty^{*3}}{3\rho c_p k_1}\left(\frac{\partial^2 T^*}{\partial y^{*2}}\right) + \frac{Q^*}{\rho C_p}(T^* - T_\infty^*) \tag{8}$$

Also, the pressure p^* inside the boundary layer is calculated by Bernoulli's pressure equation as:

$$-\frac{1}{\rho}\frac{\partial p^*}{\partial x^*} = \frac{du_\infty^*}{dt} + \left(\frac{\sigma B^2{}_0}{\rho} + \frac{\upsilon}{K^*}\right)u_\infty^* \tag{9}$$

On using (9), equation (2) become,

$$\frac{\partial u^*}{\partial t^*} + v^*\frac{\partial u^*}{\partial y^*} = \frac{du_\infty^*}{dt^*} + \nu\frac{\partial^2 u^*}{\partial y^{*2}} + g\beta_T(T^* - T_\infty^*) + g\beta_C(C^* - C_\infty^*) - \left(\frac{\sigma B^2{}_0}{\rho} + \frac{\upsilon}{K^*}\right)(u^* - u_\infty^*) \tag{10}$$

The expressions for v^* can be considered, independent of *y* and *t* as:

$$v^* = -V_0 \text{ (for suction } V_0 > 0\text{)} \tag{11}$$

We now introduce the following non-dimensional quantities as:

$$y = \frac{y^* V_0}{\upsilon},\ t = \frac{t^* V_0^2}{\upsilon},\ u = \frac{u^*}{V_0},\ u_\infty = \frac{u_\infty^*}{V_0}, v = \frac{v^*}{V_0}, Gr = \frac{g\beta_T\upsilon(T_m^* - T_\infty^*)}{V_0^3}, R = \frac{4\sigma_1 T_\infty^{*3}}{\rho c_p k_1}$$

$$Gm = \frac{g\beta_C\upsilon(C_m^* - C_\infty^*)}{V_0^3}, \omega = \frac{\omega^*\upsilon}{V_0^2}, \theta = \frac{(T^* - T_\infty^*)}{T_m^* - T_\infty^*}, S = \frac{\theta_l^*\upsilon}{\rho C_p V_0^2}, N = 1 + \frac{4R}{3}$$

$$\phi = \frac{(C^* - C_\infty^*)}{C_m^* - C_\infty^*}, \Pr = \frac{\upsilon\rho C_p}{k}, M = \frac{\sigma B_0^2\upsilon}{\rho V_0^2}, k = \frac{k^* V_0^2}{\upsilon^2}, Sc = \frac{\upsilon}{D_M}, Sr = \frac{(T_m^* - T_\infty^*)D_T}{\upsilon\left(C_m^* - C_\infty^*\right)}, F = \frac{K_l^*\upsilon}{V_0^2}$$

The corresponding non-dimensional form of equations (4), (8) and (10) are:

$$\frac{\partial u}{\partial t} - \frac{\partial u}{\partial y} = \frac{du_\infty}{dt} + \frac{\partial^2 u}{\partial y^2} + Gr\theta + Gm\phi - M_1(u - u_\infty) \tag{12}$$

$$\frac{\partial \theta}{\partial t} - \frac{\partial \theta}{\partial y} = \frac{N}{\Pr}\frac{\partial^2 \theta}{\partial y^2} + S\theta \tag{13}$$

$$\frac{\partial \phi}{\partial t} - \frac{\partial \phi}{\partial y} = \frac{1}{Sc}\frac{\partial^2 \phi}{\partial y^2} + Sr\frac{\partial^2 \theta}{\partial y^2} - F\phi \tag{14}$$

Where, $M_1 = M + \frac{1}{K}$

Subject to the non-dimensional initio - boundary conditions as:

$$\left.\begin{array}{l} u = 0, \theta = 0, \phi = 0 \text{ for every } y \text{ and } t \le 0 \\ u = 0,\ \theta = \theta_0 \exp(i\omega t), \phi = \phi_0 \exp(i\omega t),\ \text{at } y = 0 \text{ , when } t > 0 \\ \text{and } u_\infty \to A\exp(i\omega t), T \to 0, C \to 0 \text{ for } y \to \infty \text{ when } t > 0 \end{array}\right\} \tag{15}$$

4. Method of Solution

To get an exact closed form of solutions we prefer to use a set of transformations. For purely an oscillating flow, the form of solutions for the equations (12), (13) and (14) is considered as:

$$u(y,t) = \sum_{r=0}^{\infty} U_0(y)\frac{(i\omega t)^r}{r!},\ \theta(y,t) = \sum_{r=0}^{\infty}\theta_0(y)\frac{(i\omega t)^r}{r!},\ \phi(y,t) = \sum_{r=0}^{\infty}\phi_0(y)\frac{(i\omega t)^r}{r!} \tag{16}$$

On using the above set of trial solution forms (16), equations (12), (13) and (14) give,

$$\frac{d^2U_0}{dy^2}+\frac{dU_0}{dy}-(M_1+\mathrm{i}\omega)U_0=-A(M_1+\mathrm{i}\omega)-Gr\theta_0-Gm\phi_0 \tag{17}$$

$$N\frac{d^2\theta_0}{dy^2}+\Pr\frac{d\theta_0}{dy}+(S-\mathrm{i}\omega)\Pr\theta_0=0 \tag{18}$$

$$\frac{d^2\phi_0}{dy^2}+Sc\frac{d\phi_0}{dy}-(F+\mathrm{i}\omega)Sc\phi_0=-SrSc\frac{d^2\theta_0}{dy^2} \tag{19}$$

With initio-boundary conditions as:

$$\left.\begin{array}{l} U_0=0,\theta_0=0,\phi_0=0 \text{ for every } y \text{ and } t\le 0 \\ U_0=0,\theta_0=A,\phi_0=A \text{ at } y=0 \text{ when } t>0 \\ U_0\to A,\theta_0\to 0,\phi_0\to 0 \text{ for } y\to\infty \text{ when } t>0 \end{array}\right\} \tag{20}$$

The real part of expressions for non-dimensional temperature, concentration and velocity of fluid particles in the boundary layer are obtained as:

$$\theta_R(y,t)=A\exp(-\xi_1 y)\cos(\omega t-\xi_2 y) \tag{21}$$

$$\begin{aligned}\phi_R(y,t)=&\left\{(D_2\cos(\xi_4 y)+D_2\sin(\xi_4 y))\cos(\omega t)+(D_2\sin(\xi_2 y)-B_2\cos(\xi_2 y))\sin(\omega t)\right\}\exp(-\xi_1 y)\\&+\left\{(D_1\cos(\xi_4 y)+B_1\sin(\xi_4 y))\cos(\omega t)+(D_1\sin(\xi_2 y)-B_1\cos(\xi_2 y))\sin(\omega t)\right\}\exp(-\xi_3 y)\end{aligned} \tag{22}$$

$$\begin{aligned}u_R(y,t)=\{&A+(D_6\cos(\xi_6 y)+B_6\sin(\xi_6 y))\exp(-\xi_5 y)+(D_4\cos(\xi_4 y)+B_4\sin(\xi_4 y))\exp(-\xi_3 y)\\&+((D_3+D_5)\cos(\xi_2 y)+(B_3+B_5)\sin(\xi_2 y))\exp(-\xi_1 y)\}\cos(\omega t)-\{(B_6\cos(\xi_6 y)\\&-D_6\sin(\xi_6 y))\exp(-\xi_5 y)+(B_4\cos(\xi_4 y)-D_4\sin(\xi_4 y))\exp(-\xi_3 y)+((B_3+B_5)\cos(\xi_2 y)\\&-(D_3+D_5)\sin(\xi_2 y))\exp(-\xi_1 y)\}\sin(\omega t)\end{aligned} \tag{23}$$

5. Some Significant Quantities of Engineering Interest

5.1. Skin Friction at the Plate

The real part of the non-dimensional skin-friction coefficient at the plate is obtained as:

$$\tau_R=\left(\frac{\partial u}{\partial y}\right)_{y=0}=\tau_a\cos(\omega t)+\tau_b\sin(\omega t) \tag{24}$$

5.2. Rate of Heat Transfer Coefficient

The real part of the rate of heat transfer coefficient in terms of the Nusselt number is given a

$$Nu_R=-\left(\frac{\partial\theta_R}{\partial y}\right)_{y=0}=A\left(\xi_1\cos(\omega t)-\xi_2\sin(\omega t)\right) \tag{25}$$

5.3. Rate of Mass Transfer Coefficient

The real part of the mass transfer coefficient in terms of the Sherwood number is

$$Sh_R = -\left(\frac{\partial \phi_R}{\partial y}\right)_{y=0} = Sh_a \cos(\omega t) + Sh_b \sin(\omega t) \tag{26}$$

6. Results and Discussion

To investigate the influence of various physical parameters on the flow variables, numerical simulation has been made by assigning appropriate numerical values to the governing physical parameters such as magnetic field parameter (*M*), permeability parameter (*K*), Prandtl number (*Pr*), thermal Grashof number (*Gr)*, solutal Grashof number (*Gm)*, Soret number (*Sr)*, Schmidt number (*Sc)*, heat generation (source) parameter (*S*), radiation parameter (*N)*, first order chemical reaction parameter (*F*), amplitude /correction factor (*A*) and normal distances (*y*). Throughout the discussion, water is considered to be a primary fluid (solvent) and the values of Schmidt number (*Sc*) of the corresponding secondary species (solute) such as Hydrogen (H_2), Helium (*He*), Water vapor (H_2O), Oxygen (O_2) are taken as 0.22, 0.30, 0.60, 0.74 respectively and the Prandtl number (*Pr*) of the diffused fluids are taken as 7.0, which are same as the Prandtl number of water at temperature $25^{\circ}C$ or $298K$ and 1 atmosphere of pressure.

Figures 2 and 3 demonstrate the effect of heat source parameter (*S*) and radiation parameter (*N*) on the non-dimensional temperature profiles (θ_R, *y*) for a set of fixed values of *A*=0.01, ω=7.857143, ωt =1.5714, *Pr*=7.0, *N*=1.6 (fig. 1) and *S* = 0.5 (fig. 2). The parametric increase in values of *S* and *N* is found to increase the temperature of fluid particles near the plate surface, as such the temperature fluxes inside the thermal boundary layer raise, results of which, the values of Θ_R increase, while Θ_R decreases gradually to its limiting value as normal distance increases.

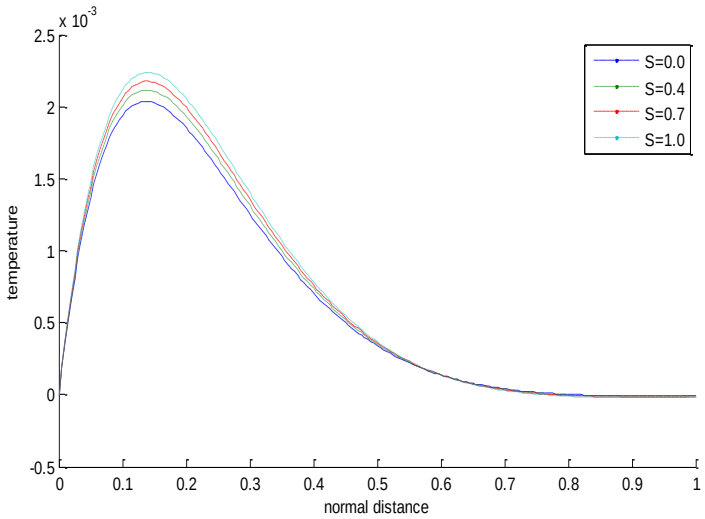

Figure 2: Temperature (θ_R) versus normal distance (*y*) for arbitrary change in values of heat source parameter (*S*).

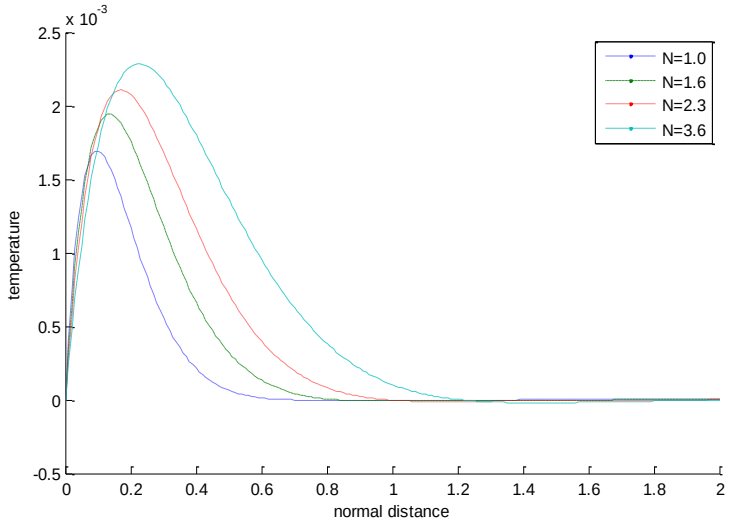

Figure 3: Temperature (θ_R) versus normal distance (y) for arbitrary change in values of radiation parameter (N).

In figures 4 to 7, the physical effect of Soret number (Sr), Schmidt number (Sc), chemical reaction parameter (F) and radiation parameter (N) on the non-dimensional concentration profiles (ϕ_R , y) are depicted for a set of fixed assigned values of A=0.01, ω=7.857143, ωt =1.5714, Pr=7.0, N=4.6 (fig. 3, 4, 5), S=0.05, Sc=0.60 (fig. 3, 5, 6), F=0.2 (fig. 3, 4, 6) and Sr = 0.15. Due to increase in parametric values of Sc, F and R, the species concentration of the fluid particles is found decreasing near the plat, while the concentration increases as Sr increases. The increase in Sc decreases the mass diffusivity, which allows the solutal boundary layer domain to shrink and thus diminishes the value of ϕ_R inside the concentration boundary layer. The mixing of the secondary fluid (solute) into the flow of primary fluid (solvent) develops a first order chemical reaction, which results in transport of mass fluxes from higher concentration zone (plate region) to the lower concentration region (free stream) thus minimizing the species concentrations near the plate surface and as such the values of ϕ_R is found to diminish gradually. Due to increase in N, the kinetic energy of the fluid particles increases, results of which increases the rate of transportation of mass fluxes. This reduces the thickness of the concentration boundary layer and diminishes the value of ϕ_R . On the other hand, as the heavier molecules of the species get separated from the lighter ones, there is a arise in the solutal boundary layer thickness, results of which, the value of ϕ_R increases due to increase in values of Sr.

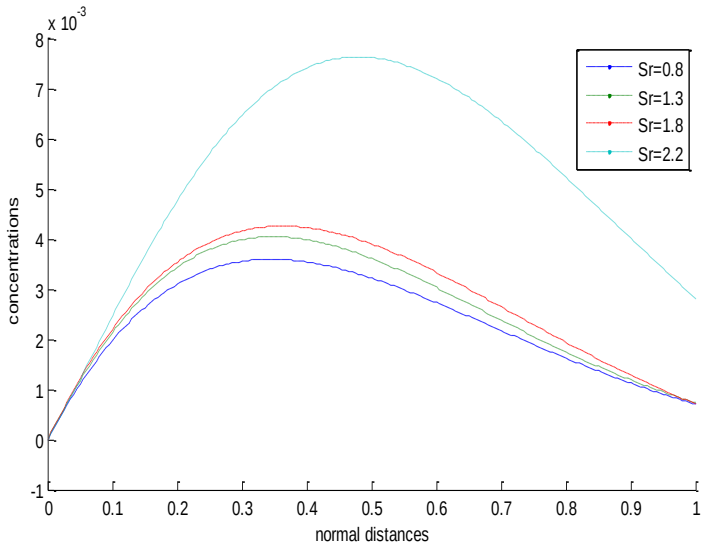

Figure 4: Concentration (ϕ_R) versus normal distance (y) for arbitrary change in values of Soret Number (Sr)

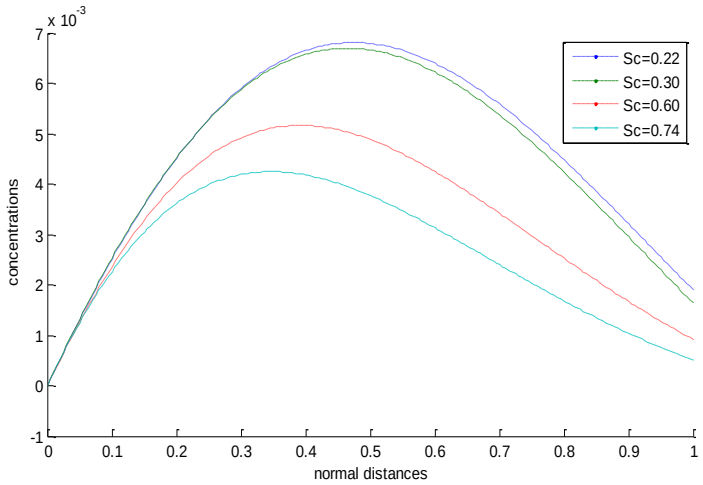

Figure 5: Concentration (ϕ_R) versus normal distance (y) for arbitrary change in values of Schmidt Number (Sc).

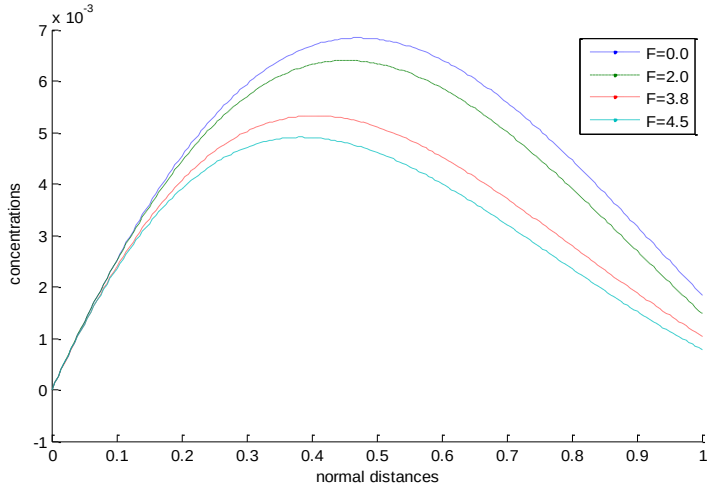

Figure 6: Concentration (ϕ_R) versus normal distance (y) for arbitrary change in values of chemical reaction parameter (F).

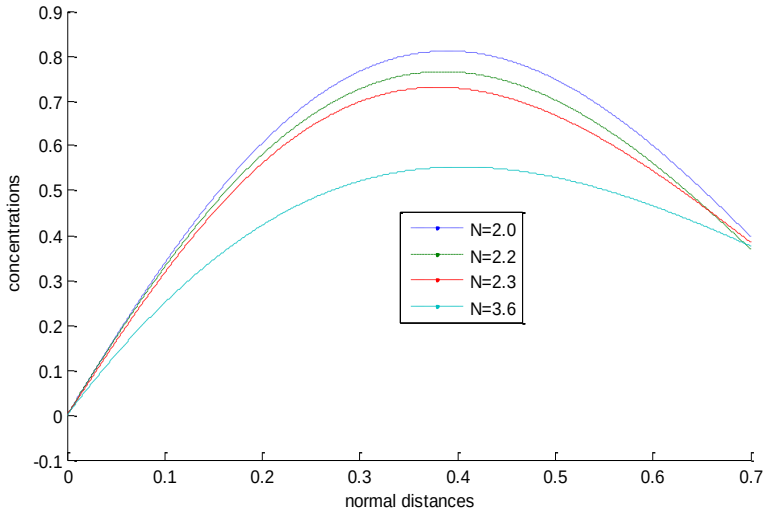

Figure 7: Concentration (ϕ_R) versus normal distance (y) for arbitrary change in values of radiation parameter (N).

The influence of Prandtl number (Pr), Soret number (Sr), radiation parameter (N) and chemical reaction parameter (F) on the main flow velocity profiles (u_R, y) is depicted in figures 8 to 11 for a set of fixed parametric values of A=1.5, N=4.0 (fig. 8, 9, 11), S=3.5, ω=7.857143, ωt =0.7857, M=0.2, K=1.5, Gr=15.0, Gm=10.0, Sc=0.22, Sr=4.0 (fig. 8, 10, 11), F=3.0 (fig. 8, 9, 10) and Sr = 4.0 (fig. 8, 10, 11) are presented graphically in figures 8, 9, 10 and 11 respectively. It is observed that for $y \in [0, 1.5)$ (approximate), the flow rate accelerates due to increase in values of Sr and N but due to an increase in Pr and F, the rate of flow is found decelerating, while for $y \geq 1.5$ (approximate) just a reversed phenomena have observed. As the value of Pr increases, the momentum diffusivity increases while the thermal diffusivity decreases, which results in decrease the kinetic energy thereby decelerates the flow rate and thus decreases the value u_R. Due to increase in Sr, the mass buoyancy force increases, which thus increase the value of u_R. The rise in values of N increases the temperature fluxes inside the boundary layer, which thus cause to increase the kinetic energy of the fluid particles. This helps to accelerate the flow rate and increases the value u_R. On the other hand, as there generates a cross flow of species due to chemical reaction, the main flow rate decelerates thus decreasing the value u_R. It is observed that, at $y \approx 0.5$, in all of the cases, the velocity picked up its highest value due to influence of thermal as well as mass buoyancy forces.

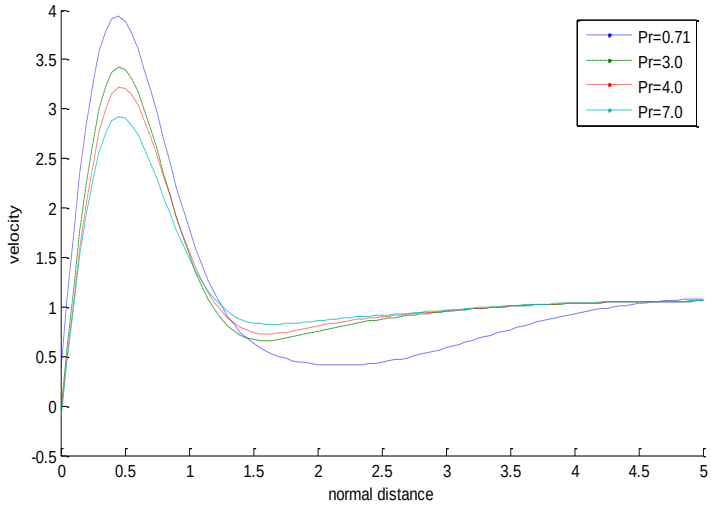

Figure 8: Velocity (u_R) versus normal distance (y) for arbitrary change in values of Prandtl number (Pr).

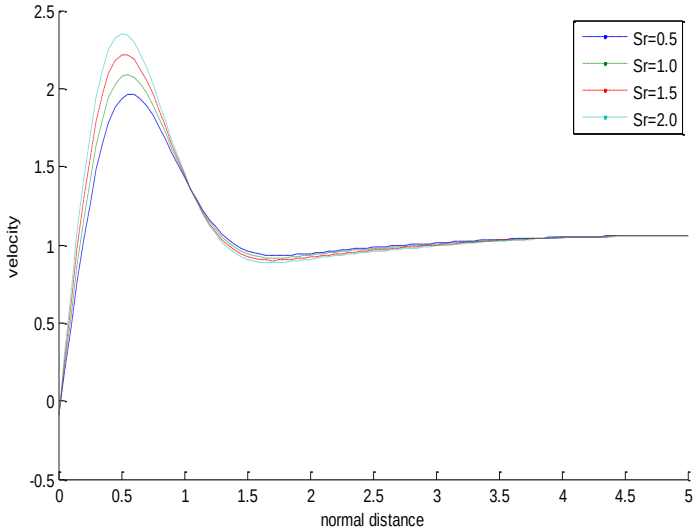

Figure 9: Velocity (u_R) versus normal distance (y) for arbitrary change in values of Soret number (Sr).

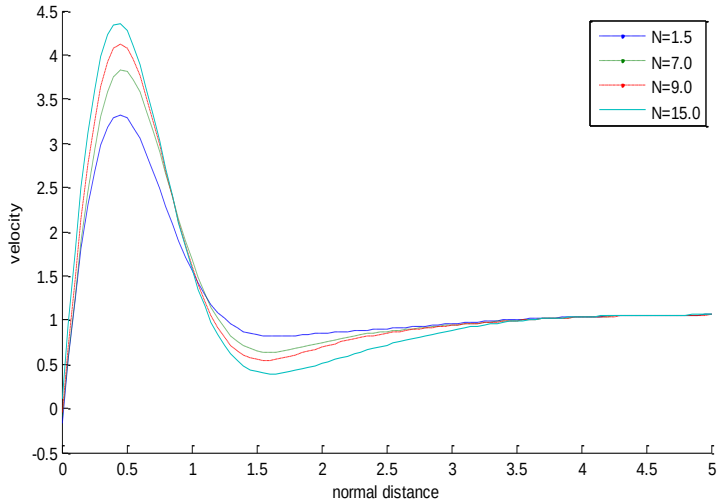

Figure 10: Velocity (u_R) versus normal distance (y) for arbitrary change in values of Radiation parameter (N).

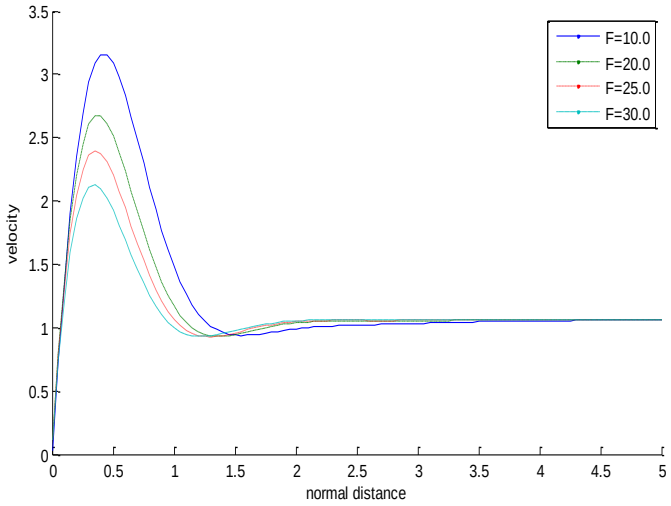

Figure 11: Velocity (u_R) versus normal distance (y) for arbitrary change in values of Chemical reaction parameter (F).

Figure 12 depicts the influence of thermal radiation parameter (N) on the Nusselt number profiles (Nu_R, S) in presence of a set of assigned values of A=0.5, Pr=7.0, t=0.1, ω=0.3. As the value of N increases, the thermal fluxes inside the thermal boundary layer increase, which increases the thickness of the thermal boundary layer as such the transport of heat fluxes decreases. This results in decelerates the heat transfer rate i.e the value of the Nusselt number decreases. The Nusselt number is initially found to increase up to $S \in [0, 2]$ (approximate) thereafter becomes constant, which indicates steady heat transfer for $S \in (2, 5]$ (approximate). Figure 13 demonstrates the presence of radiation parameter (N) on the skin-friction τ_R against time (t). As the kinetic energy of the fluid particles gets increase due to increase in radiation parameter, the rate of main flow velocity accelerates by suppressing the plate resistance as such the value of τ_R diminishes. Figure 14 shows graphically the influence of chemical reaction parameter (F) on the Sherwood number Sh_R against time (t). Due to increase in values of F, the transport of species from the higher concentration zone (plate region) to the lower concentration zone (free stream region) increases thereby accelerates the mass transfer rate form the plate region to the free stream region and as such the values of Sh_R increase.

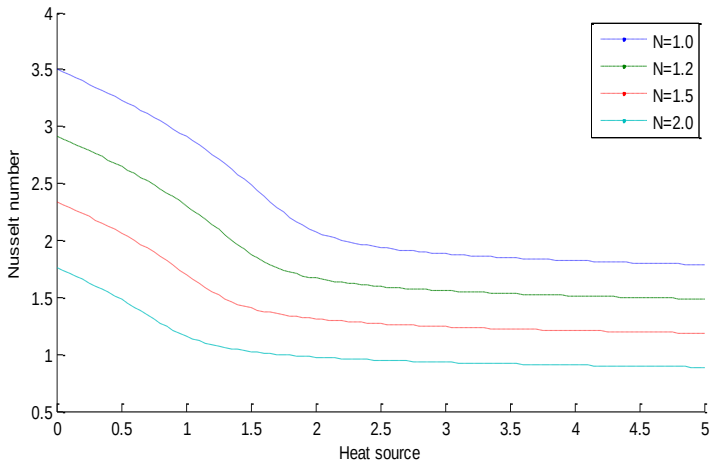

Figure 12: Nusselt number (Nu_R) versus Heat source parameter for arbitrary change in values of thermal radiation parameter (N)

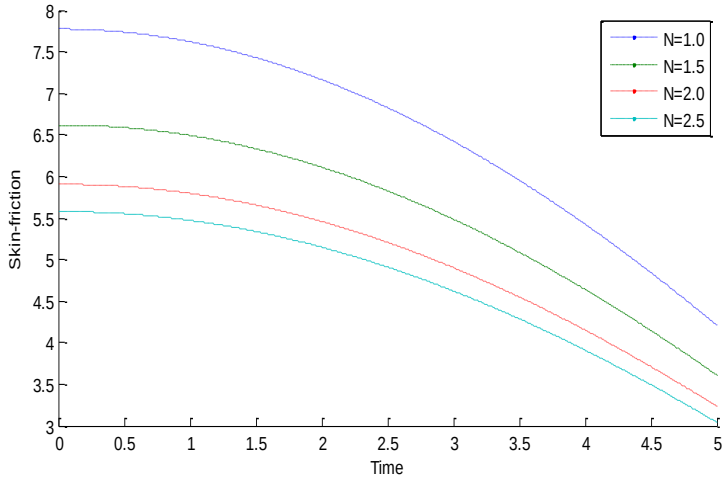

Figure 13: Skin-fraction (τ_R) versus time (t) for arbitrary change in values of thermal radiation parameter (N)

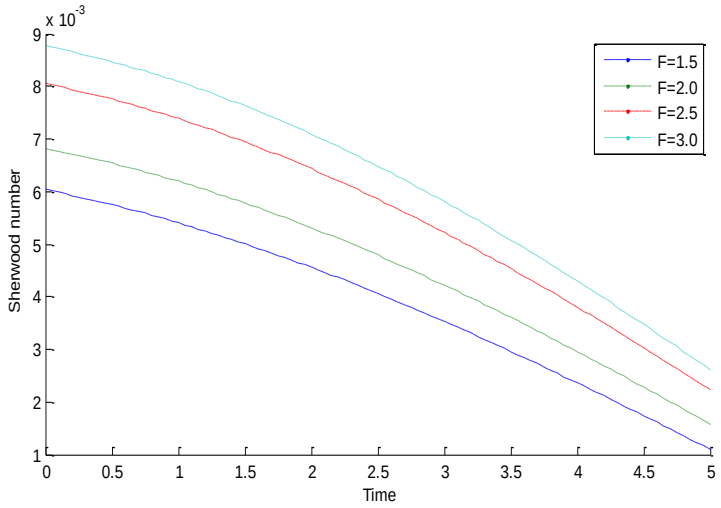

Figure 14: Sherwood number (Sh_R) versus time (t) for arbitrary change in values of Chemical reaction parameter (F).

In table 1, the variation of the numerical values of velocity against normal distances (y) and for arbitrary change in values of heat source parameter (S) is depicted for fixed parametric values of A=1.5, Pr=7.0, N=3.6, ω=7.857143 ωt =0.7857, M=0.2, K=1.5, Gr=20.0, Gm=5.0, Sc=0.22, Sr =4.0, F=3.0. It is clearly observed from the table that, the main flow velocity increases for increase in values of S, wherein the velocity is found increasing for $0 \leq y \leq 0.6$ but for $y > 0.6$ the flow rate starts decreasing gradually. Due to rise in values of S, the temperature fluxes inside the thermal boundary layer increase, which enhances the kinetic energy of the fluid particles within the flow domain, this in turn accelerates the flow rate and thus increases the values of u_R.

Table 1: The numerical values of velocity (u_R) against normal distances (y) for arbitrary variation of heat source parameter (S)

y=0	S=1.5	S=2.5	S=3.5	S=4.5
0.1	0.523084	0.511927	0.519511	0.537015
0.2	0.974627	0.979035	1.007516	1.044774
0.3	1.319549	1.346484	1.393379	1.442097
0.4	1.547827	1.593046	1.649112	1.698507
0.5	1.666757	1.721386	1.776549	1.817872
0.6	1.694310	1.749172	1.795687	1.823989
0.7	1.653560	1.701522	1.735092	1.749192
0.8	1.568318	1.605154	1.624744	1.626280
0.9	1.460067	1.484350	1.491358	1.483564
1.0	1.346152	1.358628	1.355872	1.342466

The variation in Sherwood number (Sh_R) in presence of Soret number (Sr) against heat source parameter (S) and for a set of fixed values of A=0.01, w=0.2, Pr=7.0, N=3.6, S=1.5, Sc=0.22 F=1.5, t = 0.1 is numerically shown in table 2. The mass transfer rate is being found decelerating due to increase in values of S and Sr respectively. An increase in values of S as well as Sr helps in increasing the thermal buoyancy force thus increases the longitudinal velocity and decreases the cross radial component of velocity, which thus reduces the cross radial mass transport phenomenon as such the Sherwood number decreases.

Table 2: The numerical values of Sherwood number (Sh_R) against heat source parameter (S) for arbitrary variation in values of Soret number (Sr)

S	*Sr=0.35*	*Sr=0.36*	*Sr=0.37*	*Sr=0.38*
0.00	0.009166	0.008144	0.006893	0.005602
0.02	0.009076	0.008158	0.006842	0.005617
0.04	0.008987	0.008173	0.006791	0.005632
0.06	0.008898	0.008187	0.006740	0.005647
0.08	0.008808	0.008202	0.006690	0.005663
0.10	0.008719	0.008218	0.006639	0.005679
0.12	0.008629	0.008234	0.006588	0.005695
0.14	0.008540	0.008250	0.006537	0.005711
0.16	0.008450	0.008267	0.006487	0.005728
0.18	0.008361	0.008284	0.006436	0.005745
0.20	0.008271	0.008301	0.006385	0.005763

7. Conclusions

A two dimensional unsteady mixed convective flow of a Newtonian incompressible electrically conducting fluid passed a vertical porous plate embedded in radiative heat generating Darcian porous media in presence of first order chemical reaction and Soret effect has been investigated theoretically. The governing system of equations along with a set of favorable boundary conditions is being solved analytically by normal mode method and the closed form of solutions obtained for various pertinent parameters are finally interpreted numerically through graphs and tables. The significant outcomes of the study are highlighted as follows:

- The temperature is found increasing due to increase in heat generation and thermal radiation parameters.
- The concentration of fluid particles decreases due to increase in Schmidt number and chemical reaction parameter, while the concentration increases due to increase in Soret number.
- The fluid velocity increases due to increase in Soret number, heat generation and thermal radiation parameters, but an increase in values of Prandtl number and chemical reaction parameter decreases the fluid velocity.

- The Nusselt number and the skin-fraction at the plate are found to be increased due to increase in thermal radiation parameter, while the Nusselt number initially increases due to increase in heat source parameter.
- The Sherwood number increases due to increase in chemical reaction parameter, while an increase in Soret number and heat generation parameters decreases the Sherwood number.

Acknowledgments

The authors are thankful to the Reviewers for their valuable suggestions and comments for the improvement of the quality of the paper.

Abbreviations

The following abbreviations are used in this manuscript:

A	Amplitude / Correction factor
B_0	Strength of the applied magnetic field
C_p	Specific heat at constant pressure
C^*	Species concentration
C_m^*	Mean Species concentration
C_∞^*	Species concentration in the free stream
D_M	Brownian mass diffusion co-efficient
D_T	Thermophoretic mass diffusion co-efficient
F	Chemical reaction parameter
Gm	Grashof number for mass transfer
Gr	Grashof number for heat transfer
g	Acceleration due to gravity
k	Thermal conductivity
k_1	Mean absorption co-efficient
k_l	Thermal Diffusion ratio
M	Square of the Hartmann
N	Radiation parameter
Nu_R	Nusselt number(Real part)
$p*_\infty$	Pressure in the free stream
p^*	Fluid pressure

Pr	Prandtl number
R	Thermal Radiation Parameter
S	Heat generation (source) parameter
Sc	Schmidt number
Sh_R	Sherwood number (Real part)
Sr	Soret number
T_m^*	Mean fluid temperature(dimensional)
T^*	Fluid temperature
T_m	Mean fluid temperature
T_∞^*	Temperature in the free stream
U	Free Stream velocity
(u^*, v^*)	Velocity components (dimensional)
$(u\ ,\ v)$	Velocity components (non-dimensional)
V_0	Mean suction velocity
(x^*, y^*)	Cartesian Co-ordinate (dimensional)
$(x\ ,\ y)$	Cartesian Co-ordinate (non-dimensional)

Greek Symbol

β_C	Co-efficient of solutal volume expansion
β_T	Co-efficient of thermal volume expansion
σ	Electrical Conductivity
θ	Non dimensional temperature
θ_R	Real part of θ
ϕ	Non dimensional Species Concentration
ϕ_R	Real part of ϕ
υ	Kinematic Co-efficient of viscosity
ω	Frequency of Oscillation
τ_R	Real part of non dimensional skin friction coefficient
v^*	Suction velocity
ρ	Fluid density
ρ_∞	Free stream fluid density

Subscripts:

m	Conditions on the wall
∞	Free stream condition

References

[1] Ahmed M, Sarki N., Radiation Effects on Heat and Mass Transfer over an Exponentially Accelerated Infinite Vertical Plate with Chemical Reaction, *Proceedings of the International Multi Conference of Engineers and Computer Scientists, IMECS, Hong Kong*, 2(2014): 12–14.

[2] Ahmed N, Sengupta S and Datta D., An exact analysis for MHD free convection mass transfer flow past an oscillating plate embedded in a porous medium with Soret effect, *Chem. Engg. Comm*., 200(2013): 494–513.

[3] Ananda Reddy N, Varma S.V.K and Raju M.C., Thermo diffusion and chemical effects with simultaneous thermal and mass diffusion in MHD mixed convection flow with Ohmic heating, *Journal of Naval Architecture and Marine Engineering*, 6(2)(2009): 84–93.

[4] Babu P R, Rao J A and Sheri S., Radiation Effect on MHD Heat and Mass Transfer Flow over a Shrinking Sheet with Mass Suction, *Journal of Applied Fluid Mechanics*, 7(4) (2014) : 641–650.

[5] Beckett P M, Friend I E. Combined natural and forced convection between parallel walls developing flow at higher Rayleigh numbers, *International Journal of Heat and Mass Transfer*, 27(1984): 611-621.

[6] Bhattacharyya K., Effects of radiation and heat source/sink on unsteady MHD boundary layer flow and heat transfer over a shrinking sheet with suction/injection, *Frontiers of Chemical Engineering in China*, 5(3) (2011): 376–384.

[7] Chamkha A J., MHD flow of a numerical of uniformly stretched vertical permeable surface in the presence of heat generation/ absorption and a chemical reaction. *Int. Comm. Heat Mass Transfer, 30*(2003): 413–422.

[8] Chandra Reddy P., Raju M.C. and Raju G. S. S., Soret and Dufour effects on MHD free convection flow of Rivlin-Ericksen fluid past a semi-infinite vertical plate, *Advances and Applications in Fluid Mechanics*, 19 (2) (2016): 401-414.

[9] England W G, Emery A F., Thermal radiation effects on the laminar free convection boundary layer of an absorbing gas. *J. Heat Trans.* 91(1969): 37–44.

[10] Imran A, Abdul R, Mohd K, Zulkibri I, Mohd Z S, Sharidan S., Chemical Reaction and Uniform Heat Generation or Absorption Effects on MHD Stagnation-Point Flow of a Nanofluid over a Porous Sheet, *World Applied Sciences Journal*, 24 (10) (2013): 1390–1398.

[11]Kesavaiah D, Satyanarayana P V,Venkataramana S., Effects of the chemical reaction and radiation absorption on an unsteady MHD convective heat and mass transfer flow past a semi-infinite vertical permeable moving plate embedded in a porous medium with heat source and suction. *Int. J. of Appl. Math and Mech,* 7 (1) (2011):52–69.

[12] Kuhn S., Rohr P.R.V., Experimental investigation of mixed convective flow over a wavy wall, *International Journal of Heat and Fluid Flow,* 29(2008): 94–106.

[13] Magyari E and Pentokratoras A., Note on the effect of thermal radiation in the linearized Rosseland approximation on the heat transfer characteristics of various boundary layer flow. *Int. commun. heat and mass transfer*, 38(2011): 554 – 556.

[14] Mamatha B. ,Raju M.C.and Varma S.V.K.,Thermal diffusion effect on MHD mixed convection unsteady flow of a micro polar fluid past a semi-infinite vertical porous plate with radiation and mass transfer, *International Journal of Engineering Research in Africa,* 13 (2015):21–37.

[15] Muthtamilselvan M, Prakash D, Doh D H., Effect of Non-Uniform heat Generation on unsteady MHD flow over a vertical stretching surface with variable thermal conductivity, *Cambridge journal of mechanics*, 30(02) (2014): 199–208.

[16] Muthtamilselvan M, Prakash D, Doh D H, Effect of Non-Uniform Heat Generation on Unsteady MHD Non-Darcian Flow over a Vertical Stretching Surface with variable Properties, *Journal of Applied Fluid Mechanics*, 7(3) (2014): 425–434.

[17] Pal D, Talukdar B., Combined effects of Joule heating and chemical reaction on unsteady magnetohydrodynamic mixed convection of a viscous dissipating fluid over a vertical plate in porous media with thermal radiation, *Mathematical and Computer Modelling,* 54(2011): 3016–3036.

[18] Pandya N, Shukla A K., Soret-Dufour and Radiation Effects on Unsteady MHD Flow past an Impulsively Started Inclined Porous Plate with Variable Temperature and Mass Diffusion, *International journal of mathematics and scientific computing,* 3(02) (2013) : 41–48.

[19] Prakash J, Ogulu A., Unsteady two-dimensional flow of a radiating and chemically reacting MHD fluid with time-dependent suction, *Indian Journal of Pure and Applied physics, 44*(2006): .805-810.

[20] Rajesh V, Varma S V K., Radiation effects on MHD flow through a porous medium with variable temperature or variable mass diffusion, *IJAMM,* 6(1) (2010): 39–57.

[21] Raju M.C., Chamkha A.J., Philip J. and Varma S.V.K., Soret Effect Due to Mixed Convection on Unsteady Magnetohydrodynamic Flow Past a Semi Infinite Vertical Permeable Moving Plate in Presence of Thermal Radiation, Heat Absorption and Homogenous Chemical Reaction, *International Journal of Applied Computational Mathematics*,1(1) (2016):1–15.

[22]Raju M. C .and Varma S.V.K., Soret effects due to natural convection in a non-Newtonian fluid

flow in porous medium with heat and mass transfer, *Journal of Naval architecture and Marine Engineering,*11 (2) (2014): 147–156.

[23]Raju M.C, Varma S.V.K., Reddy P.V. and Saha S., Soret effects due to Natural convection between Heated Inclined Plates with Magnetic Field, *Journal of Mechanical Engineering,* 39(2) (2008): 43–48.

[24] Ram P C., Heat and mass transfer on MHD heat generating flow through a porous medium in a rotating fluid, *Springer Astrophysics and space Sci,*172(1990): 273–277.

[25] Seddeek M A, Almushigeh A A., Effects of radiation and variable viscosity on MHD free convective flow and mass transfer over a stretching sheet with chemical reaction, *Applications and Applied mathematics,* 5 (1) (2010): 181–7197.

[26] Sengupta S., Thermal diffusion effect of free convection mass transfer flow past a uniformly accelerated porous plate with heat sink. *International Journal of Mathematical Archive,* 2(8) (2011): 1266–1273.

[27] Sengupta S., Free Convective Chemically Absorption Fluid Past an Impulsively Accelerated Plate with Thermal Radiation Variable Wall Temperature and Concentrations, *Applications and Applied Mathematics,* 10(1) (2015): 328 –348.

[28] Sengupta S., An Analysis on Unsteady Heat and Mass Transfer Flow of Radiative Chemically Reactive Fluid past an Oscillating Plate Embedded In Porous Media in Presence of Soret Effect, *International Journal of Recent Technology and Engineering,* 3(6) (2015): 10–14.

[29] Sengupta S, Ahmed N., Chemical reaction interaction on unsteady MHD free convective radiative flow past an oscillating plate embedded in porous media with thermal diffusion, *Advances in Applied Science Research,* 6(7) (2015): 87–104.

[30] Sengupta S and Sen M., Free convective heat and mass transfer flow past an oscillating plate with heat generation, thermal radiation and thermo diffusion effects. *J.P J. of heat and mass transfer,* 8(2) (2013): 187–210.

[31] SudheerBabu M, Satyanarayana P V., Effects of the chemical reaction and radiation absorption on free convection flow through porous medium with variable suction in the presence of uniform magnetic field, *J.P. Journal of Heat and Mass Transfer, 3*(2009): 219–234.

Appendix A

$$\xi_1=\frac{1}{2N}\left[\mathrm{Pr}+\frac{\sqrt{\mathrm{Pr}}}{\sqrt{2}}\left[\sqrt{(\mathrm{Pr}-4NS)+\sqrt{(\mathrm{Pr}-4NS)^2+16N^2\omega^2}}\right]\right] \qquad \xi_2=\frac{1}{2N}\left[\frac{\sqrt{\mathrm{Pr}}}{\sqrt{2}}\left[\sqrt{\sqrt{(\mathrm{Pr}_r-4NS)^2+16N^2\omega^2}-(\mathrm{Pr}-4NS)}\right]\right]$$

$$\xi_3=\frac{1}{2}\left[Sc+\frac{\sqrt{Sc}}{\sqrt{2}}\left[\sqrt{(Sc+4F)+\sqrt{(Sc+4F)^2+16\omega}}\right]\right] \qquad \xi_4=\frac{1}{2}\left[\frac{\sqrt{Sc}}{\sqrt{2}}\left[\sqrt{\sqrt{(Sc+4F)^2+16\omega}-(Sc+4F)}\right]\right]$$

$$\xi_5=\frac{1}{2}\left[1+\frac{1}{\sqrt{2}}\left[\sqrt{4M_1+\sqrt{(4M_1+1)^2+16\omega^2}}\right]\right] \qquad \xi_6=\left[\frac{1}{2\sqrt{2}}\left[\sqrt{\sqrt{(4M_1+1)^2+16\omega^2}-(4M_1+1)}\right]\right]$$

$$d_1=\xi_1^2-\xi_2^2-Sc\xi_1-FSc,\ d_2=2\xi_1\xi_2-Sc\xi_2-\omega Sc,\ d_3=\xi_1^2-\xi_2^2-\xi_1-M_1,\ d_4=2\xi_1\xi_2-\xi_2-\omega,\ d_5=\xi_3^2-\xi_4^2-\xi_3-M_1,$$

$$d_6=2\xi_3\xi_4-\xi_4-\omega,\ a_1=d_1\left(\xi_1^2-\xi_2^2\right),\ a_2=d_2\left(2\xi_1\xi_2\right),\ D_1=\frac{-AaScSr_1}{d_1^2+d_2^2},\ B_1=\frac{-Aa_2ScSr}{d_1^2+d_2^2},\ D_2=A-D_1,\ D_3=-\frac{Ad_3Gr}{d_3^2+d_4^2},$$

$$D_4=\frac{-Gm\left(D_2d_5+B_2d_6\right)}{d_5^2+d_6^2},\ D_5=\frac{-Gm\left(D_1d_3+B_1d_4\right)}{d_3^2+d_4^2},\ D_6=-A-D_3-D_4-D_5,\ B_2=-B_1,\ B_3=\frac{Ad_4Gr}{d_3^2+d_4^2},\ B_4=\frac{Gm\left(D_2d_6-B_2d_5\right)}{d_5^2+d_6^2},$$

$$B_5=\frac{Gm\left(D_1d_4-B_1d_3\right)}{d_3^2+d_4^2},\ B_6=-B_3-B_4-B_5,\ Sh_a=D_1\xi_1-B_1\xi_4+D_2\xi_3-B_2\xi_4,\ Sh_b=-B_1\xi_1-D_1\xi_2-B_2\xi_3-D_2\xi_2,$$

$$\tau_a=-\left(D_4+D_5\right)\xi_1+\left(B_3+B_5\right)\xi_2-D_4\xi_3+B_4\xi_4-D_6\xi_5+B_6\xi_6$$

$$\tau_b=\left(B_3+B_5\right)\xi_1+\left(D_3+D_5\right)\xi_2+B_4\xi_3+D_4\xi_4+B_6\xi_5+D_6\xi_6$$